Impaired fetal brain growth and neurodevelopmental deficits at 2 years: deep phenotyping of maternal–fetal pathophysiology

José Villar, Maria Carvalho, Robert Gunier, Rose McGready, Yolotzin Valdespino, Kim A Lagerborg, Fernando C Barros, Agustin Conde-Agudelo, Shane A Norris, Michelle Fernandes, Antonio Uttaro, Taylor W Carter, Rafael E Valentin, Ge Zhang, Shama Munim, Stephen Rauch, Madeleine K Wyburd, James A Berkley, Manu Vatish, Verena I Carrara, Rachel Craik, Hellen C Barsosio, Leila Cheikh Ismail, Chrystelle O O Tshivuila-Matala, Roseline Ochieng, Eric O Ohuma, Alan Stein, Ann Lambert, Ana Namburete, Adele Winsey, Louis J Muglia, Brenda Eskenazi, Neil J Sebire, Dayle L Sampson, Zulfiqar A Bhutta, Lee D Roberts, Aris T Papageorghiou*, Stephen H Kennedy**

Lancet Obstet Gynaecol Womens Health 2026; 2: e310–23

See **Comment** page e268

*Contributed equally

Nuffield Department of Women's & Reproductive Health, University of Oxford, Oxford, UK (Prof J Villar MD, Y Valdespino MD, M Fernandes MD, Prof M Vatish MD, R Craik BSc, C O O Tshivuila-Matala DPhil, Prof E O Ohuma DPhil, A Lambert PhD, A Winsey PhD, Prof A T Papageorghiou MD, Prof S H Kennedy MD); **Oxford Maternal & Perinatal Health Institute, Green Templeton College, University of Oxford, Oxford, UK** (Prof J Villar, Y Valdespino, A Conde-Agudelo PhD, A Lambert, Prof A T Papageorghiou, Prof S H Kennedy); **Department of Obstetrics & Gynaecology** (M Carvalho MD), **Faculty of Health Sciences, Aga Khan University Hospital, Nairobi, Kenya** (R Ochieng MMED); **Center for Environmental Research and Community Health, School of Public Health, University of California, Berkeley, CA, USA** (R Gunier PhD, S Rauch MPH, Prof B Eskenazi PhD); **Centre for Tropical Medicine and Global Health** (Prof R McGready MD, Prof J A Berkley FRCPCH, V I Carrara MD), **Wellcome Centre for Human Genetics, Nuffield Department of Medicine, University of Oxford, UK** (Prof M Vatish); **Shoklo Malaria Research Unit, Mahidol-Oxford Tropical Medicine Research Unit, Faculty of Tropical Medicine, Mahidol University, Mae Sot, Thailand** (Prof R McGready, V I Carrara); **Sapient Bioanalytics, San Diego, CA, USA** (K A Lagerborg PhD);

Summary

Background Impaired fetal cranial growth trajectories, diverging before 20 weeks' gestation, are associated with growth, vision, and neurodevelopment deficits at age 2 years. We aimed to understand the maternal–fetal pathophysiological processes underlying childhood developmental deficiencies.

Methods Between 2012 and 2019, the INTERBIO-21st Fetal Study enrolled 3598 pregnant women who initiated antenatal care before 14 weeks' gestation. We prospectively measured fetal cranial and linear growth and brain volume, and we monitored the infants' health, growth, and development from birth to age 2 years to identify growth and development phenotypes. We grouped the observed cranial growth into five distinct phenotypes: median growth tracking (MGT; steady growth throughout pregnancy, close to the INTERGROWTH-21st 50th centile); early faltering growth (EFG; growth faltered throughout pregnancy); late faltering growth (LFG; higher but parallel growth to the MGT trajectory through the second trimester, with growth starting to falter by the early third trimester); accelerating growth (AG; growth close to the 50th centile through the second trimester followed by accelerated growth during the third trimester); and late median growth tracking (LMG; accelerated growth post 15 weeks' gestation, followed by a normalising growth rate in the third trimester). These phenotypes were associated with distinct growth, vision, and developmental outcomes at age 2 years. We also prospectively and concomitantly obtained early pregnancy maternal blood samples, measured maternal–fetal placental blood flow, and collected placental tissue and umbilical cord blood samples at birth. In this study, we did placental histopathology, and genetic, epigenetic, and metabolomic wide association studies to better understand the pathophysiology of fetal phenotypes that manifest distinct characteristics in childhood.

Findings We first explored the association between the previously identified fetal head circumference phenotypes, as described above, and placental physiology, metabolomic, and genetic outputs. The most severe growth and development deficiency was observed in the cranial EFG phenotype, which demonstrated fetal growth restriction before 25 weeks' gestation. It was associated with reduced umbilical cord blood flow and an increased maternal vascular malperfusion compared with the other four phenotypes. The EFG phenotype had a phospholipid signature with odds ratios (ORs) of 1·42 (95% CI 1·32–1·51) for phosphatidylcholine (PC) and of 1·41 (1·32–1·50) for ether lipids PC (O-) species associated with the EFG group in maternal samples at less than 16 weeks' gestation rather than plasmologens; there were also positive ORs for early maternal oxidised PC signatures (OR 1·41; 1·32–1·50), in a reciprocal pattern with the AG phenotype. There was a consistent epigenetic hypermethylation pattern in umbilical cord samples of peroxisomal genes *PEX 10* and *14* and of genes encoding enzymes within the plasmalogen pathway (*FASN*, *GNPAT*, and *PEDS 1*); hypomethylation of the *FAR1* gene (encoding the rate-limiting enzyme); and epigenetic hypermethylation of *CPT1* and *ACSL1* suggestive of impaired fetal fatty acid β-oxidation.

Interpretation We provided placental, epigenetic, and molecular characterisation of the pathophysiology underlying early fetal cranial and brain volume impaired growth, with consistency between epigenetic and metabolomic results. These mechanisms appear to exert cumulative downstream growth and developmental influences into childhood.

Funding The Bill & Melinda Gates Foundation.

Introduction

The maternal–fetal exposome has long-lasting effects on a child's subsequent health, growth, neurodevelopment, emotional and social interactions, educational attainment, and income.[1,2] However, the pathophysiology, interlinked influences and timing of exposures, and domain specificity of neurodevelopmental impairment remain unclear.

Research in context

Evidence before this study

Our systematic review identified 28 metabolomic studies that assessed the pathophysiology of intrauterine growth restriction (IUGR) and small for gestational age (SGA) in maternal blood, umbilical cord blood, or both. Of the 19 studies using maternal blood, none of which evaluated fetal growth trajectories nor neurodevelopment, only five took samples from pregnancies at 20 weeks' gestation or earlier. The two largest studies reported dissimilar results. A study of 878 women, with 98 newborn babies SGA and 780 newborn babies appropriate for gestational age, found no significant differences in maternal amino acids, non-esterified fatty acids, phospholipids, or carnitines. However, a study of 474 women, with 175 term newborn babies with IUGR and 299 controls, found most steroid pathway metabolites were downregulated and metabolites related to the plasmalogen pathway were upregulated. Of the 21 metabolomic studies in cord blood, only one included postnatal follow-up, and only four included more than 50 newborn babies with IUGR or SGA. Most reported significant differences in amino acids, lysophosphatidylcholines, phosphatidylcholines (PCs), and carnitine, although the direction of the association varied. For example, phenylalanine was upregulated in four and downregulated in two studies; alanine was upregulated in three and downregulated in two studies; glutamine was upregulated in two and downregulated in two studies; and valine, isoleucine, and carnitine were all upregulated in three and downregulated in one study. Most PCs and lysophosphatidylcholines were downregulated, whereas the remaining metabolites showed an inconsistent trend.

Added value of this study

We have previously defined a fetal phenotype consisting of early faltering growth (EFG) of the cranium associated with impaired growth, vision, and neurodevelopment at age 2 years. In this study, we have refined the phenotype by showing its association to: (1) a set of maternal risk factors, nutritional biomarkers, and pregnancy complications; (2) a hypoxic placental environment, defined by increased umbilical artery Doppler pulsatility index trajectories from 22 weeks' gestation measured concomitantly with cranial growth, and histopathological evidence of maternal vascular malperfusion; (3) faltering volumetric growth of the fetal brain between 14 and 31 weeks' gestation, without evidence of a significant genetic association with large effect; (4) robust hypermethylation and hypomethylation patterns in cord plasma; and (5) highly specific maternal–fetal metabolic signatures based on an untargeted metabolomic analysis of linked maternal early pregnancy and cord samples. We found an over-representation in maternal plasma of the ether-bonded alkyl-acyl phospholipids (PC-O; rather than plasmalogens) and canonical PC species (rather than phosphatidylethanolamines) in the EFG phenotype. We also found evidence of alterations in fatty acid β-oxidation, in cord plasma, based on a reciprocal pattern of metabolite signatures between the EFG (downregulated) and accelerating growth phenotypes. Finally, we found evidence of hypermethylation of *PEX* genes 10 and 14, which encode proteins directly involved in peroxisome membrane traffic, with downstream hypermethylation of genes encoding several key enzymes in the plasmalogen biosynthesis pathway, consistent with regulatory disruption at the epigenetic rather than genetic level.

Implications of all the available evidence

We have identified disruption in maternal and fetal metabolic pathways associated with EFG of the fetal cranium and brain, which results in poor infant growth and neurodevelopmental outcomes. To our knowledge, no previous study has investigated large numbers of mother–infant dyads from early pregnancy to childhood, while concomitantly exploring such a wide-ranging set of variables and molecular pathways. We followed an untargeted metabolomic approach that led to a focused epigenetic analysis of the relevant glycerophospholipid biosynthesis pathways. Our findings suggest a biological association indicative of fundamental processes regulating human fetal growth and could lead to biomarkers for the risk of developmental delay.

The INTERGROWTH-21st Project has shown that, when maternal health, educational, environmental, and nutritional needs are met, fetal growth, brain maturation, and newborn size and body composition are consistently similar across diverse populations and geographies,[3–5] with satisfactory growth, neurodevelopment, and associated behaviours at age 2 years.[6,7] Conversely, in medium-to-high-risk pregnancies in the INTERBIO-21st Fetal Study, we identified five distinct phenotypes of cranial growth: median growth tracking (MGT; for steady growth throughout pregnancy, close to the INTERGROWTH-21st 50th centile); early faltering growth (EFG; for growth faltered throughout pregnancy); late faltering growth (LFG; for higher but parallel growth to the MGT trajectory through the second trimester, with growth starting to falter by the early third trimester); accelerating growth (AG; for growth close to the 50th centile through the second trimester followed by accelerated growth during the third trimester); and late median growth tracking (LMG; for accelerated growth post 15 weeks' gestation followed by a so-called normalising growth rate in the third trimester). EFG of the fetal cranium, starting between 20 and 25 weeks' gestation,[8] is inversely associated with growth, cognitive, fine motor, language, and vision development at age 2 years.[9]

We now explore the biology of these early fetal cranial and brain volume growth phenotypes that track with postnatal growth, vision, and development until age 2 years. Across these phenotypes, we investigated: (1) patterns of placental blood flow and histopathological malperfusion; (2) maternal and fetal genetic variants;

Programa de Pós-Graduação em Saúde e Comportamento, Universidade Católica de Pelotas, Pelotas, Brazil (Prof F C Barros MD); **SAMRC Developmental Pathways For Health Research Unit, Department of Paediatrics & Child Health, University of the Witwatersrand, Johannesburg, South Africa** (Prof S A Norris PhD, C O O Tshivuila-Matala); **Faculty of Medicine, Department of Paediatrics, University of Southampton, Southampton, UK** (M Fernandes); **Instituto de Biología Molecular y Celular de Rosario, Consejo Nacional de Investigaciones Científicas y Técnicas, Rosario, Argentina** (Prof A Uttaro PhD); **Elysium Health, New York, NY, USA** (T W Carter MSc, R E Valentin PhD, D L Sampson PhD); **Division of Human Genetics, Cincinnati Children's Hospital Medical Center, Cincinnati, OH, USA** (Prof G Zhang PhD, Prof L J Muglia PhD); **Center for Prevention of Preterm Birth, Perinatal Institute, Cincinnati Children's Hospital Medical Center and March of Dimes Prematurity Research Center Ohio Collaborative, Cincinnati, OH, USA** (Prof G Zhang); **Department of Pediatrics, University of Cincinnati College of Medicine, Cincinnati, OH, USA** (Prof G Zhang); **Department of Obstetrics and Gynaecology, Division of Women and Child Health, Aga Khan University, Karachi, Pakistan** (Prof S Munim MD); **Oxford Machine Learning in Neuroimaging laboratory (OMNI), Department of Computer Science, University of Oxford, Oxford, UK** (M K Wyburd DPhil, Prof A Namburete DPhil); **Wellcome Centre for Integrative Neuroimaging, FMRIB, Nuffield Department of Clinical Neurosciences, University of Oxford, Oxford, UK** (M K Wyburd, Prof A Namburete); **KEMRI/Wellcome Trust Research Programme, Kenya** (Prof J A Berkley); **KEMRI-Coast Centre for Geographical Medicine and Research, University of Oxford, Kilifi, Kenya** (H C Barsosio MD); **Clinical Nutrition and Dietetics Department, University of Sharjah, Sharjah, United Arab**

Emirates (L Cheikh Ismail PhD); **Health, Nutrition & Population Global Practice, World Bank Group, Washington, DC, USA** (C O O Tshivuila-Matala); **Maternal, Adolescent, Reproductive & Child Health (MARCH) Centre, London School of Hygiene & Tropical Medicine, London, UK** (Prof E O Ohuma); **Blavatnik School of Government, University of Oxford, Oxford, UK** (Prof A Stein FRCPsych); **MRC/Wits Rural Public Health and Health Transitions Research Unit (Agincourt), School of Public Health, Faculty of Health Sciences, University of the Witwatersrand, Johannesburg, South Africa** (Prof A Stein); **African Health Research Institute, Nelson R Mandela School of Medicine, Durban, South Africa** (Prof A Stein); **Burroughs Wellcome Fund, Durham, NC, USA** (Prof L J Muglia); **National Institute for Health and Care Research Great Ormond Street Hospital Biomedical Research Centre at UCL, London, UK** (Prof N J Sebire MD); **Center for Global Child Health, Hospital for Sick Children, Toronto, ON, Canada** (Prof Z A Bhutta MD); **Institute for Global Health and Development, Aga Khan University, Karachi, Pakistan** (Prof Z A Bhutta); **Leeds Institute of Cardiovascular and Metabolic Medicine, University of Leeds, Leeds, UK** (Prof L D Roberts PhD)

Correspondence to: Prof José Villar, Nuffield Department of Women's & Reproductive Health, University of Oxford, Women's Centre, John Radcliffe Hospital, Oxford OX3 9DU, UK
jose.villar@wrh.ox.ac.uk

See **Online** for appendix 1

(3) maternal early pregnancy and fetal metabolomic signatures; and (4) the epigenetic regulation of the fetal genes encoding the enzymes of the observed metabolic pathways.

Methods

Study design, participants, and samples

This prospective, observational study was done in multiple centres in six countries: all four maternity hospitals in Pelotas (Brazil), the urban Aga Khan University Hospital in Nairobi (Kenya), the rural Kilifi County Hospital (Kenya), AKUH teaching hospital in Karachi (Pakistan), Chris Hani Baragwanath Academic Hospital in Johannesburg (South Africa), the only government hospital serving all of Soweto (South Africa), the Shoklo Malaria Research Unit in Mae Sot (Thailand), and the Oxford University Hospitals in Oxford (UK), between Feb 8, 2012, and Nov 30, 2019.[9,10]

The INTERBIO-21st Study and its ancillary studies were approved by the Oxfordshire Research Ethics Committee 'C' (reference: 08/H0606/139), the research ethics committees of the individual participating institutions, as well as the corresponding regional health authorities where the project was implemented.

We enrolled 3598 women who initiated antenatal care at less than 14 weeks' gestation,[11] determined by ultrasound dating,[12] irrespective of their pregnancy risk profile (ie, an unselected population). We excluded women younger than 18 years, with a BMI higher than 35 kg/m² (to facilitate fetal ultrasound scanning), assisted conception, and multiple pregnancy.[11] We monitored their pregnancies to delivery, and their children's health, growth, and development until age 2 years; corrected age was used for infants born preterm.[13] All mothers provided written informed consent for the use of their clinical data and biological samples.

The appendix 1 (pp 2–4) summarises the methodology, previously reported, to identify the fetal phenotypes (including data management, ultrasound scanning, clinical information, anthropometry, and neuro-developmental assessment at age 2 years).[11,14–22]

From the eligible cohort of 3206 women who had three or more fetal ultrasound scans, we selected 2655 women who also provided venous blood samples (who were non-fasting, in line with recent publications[23–25]) at a median gestational age of 13·2 weeks (IQR 11·9–17·2). From 2429 of these women, we collected umbilical cord venous blood samples within 30 min of delivery and two placental samples (approximately 8 mm diameter × full placental thickness) within 1 h of delivery, if possible (appendix 1 p 5).

To investigate the pathophysiological processes underlying the EFG phenotype, we measured uterine artery and umbilical cord blood flow, and examined placental histopathology, as proxies for oxygenation and nutrient transfer, and used the maternal and cord blood samples to: (1) conduct genome-wide association studies (GWAS) to identify maternal and fetal genetic variants; (2) explore metabolomic signatures associated with the phenotypes, and (3) conduct an epigenome-wide association study (EWAS) focused on the fetal methylation patterns related to the metabolic pathways suggested by metabolomics.

Metabolomic analyses

The detailed methodology related to rapid liquid chromatography–mass spectrometry and spectral data handling, extraction, and alignment is presented in the appendix 1 (p 6). This method of tandem mass spectrometry (MS/MS) aimed to provide detailed structural information on the makeup of molecules. We conducted logistic regression analysis to identify metabolite features associated with the fetal phenotypes, controlling for maternal age and newborn sex (glm function from R, family=binomial, link=logit).

Metabolite features were standardised to a z-score by subtracting the mean and scaling to unit variance with the standard score of metabolite feature x calculated as $z=(x-u)/s$ where u is the mean and s is the SD of the metabolite abundances. A single metabolome-wide significance threshold of p lower than 1×10^{-6} was used to identify the principal associated metabolite features, a significance level empirically determined using a rough estimate of the independent number of metabolite features in a typical dataset. The output was the odds ratio (OR) for the metabolite, calculated by exponentiation of the estimate of the coefficient of the variable of interest, metabolite level, from the logistic regression model. These ORs should be interpreted as the odds of being in the EFG phenotype (or AG phenotype) compared with the odds of being in the MGT phenotype.

To visualise how metabolites associated with the two most divergent phenotypes diverged at the metabolome-wide level, we performed a supervised Uniform Manifold Approximation and Projection (UMAP) using the significant metabolites, with their intensities being imputed using the minimum value and then z-scaled.

Sample preparation and laboratory methods for the EWAS and GWAS are described in detail in the appendix 1 (pp 9–10).

Statistical analysis

Differential methylation analysis was conducted using the limma package (version 3.58.1) in R (version 4.3.1) to identify differentially methylated positions between phenotypes. A linear modelling framework was used, specifying a design matrix that included phenotype indicators and covariates for gestational age at birth, maternal age, and newborn sex.

Pairwise contrasts between phenotypes were then defined using makeContrasts to extract specific comparisons, followed by model fitting with lmFit() and

contrast fitting using contrasts.fit(). We applied variance moderation using eBayes,[26] which implements an empirical Bayes shrinkage of standard errors, improving inference stability across the numerous CpG sites interrogated.

We applied the Benjamini–Hochberg procedure (adjust.method="BH" parameter in topTable) to account for the multiple testing inherent in genome-wide methylation data, controlling the false discovery rate. Significant differentially methylated positions were identified at an adjusted p value threshold of 0·05 or lower.

Results were visualised using volcano plots, with $\log_2$ fold changes on the x-axis (with a threshold at ±0·585, equivalent to a 1·5-fold change) and $-\log_{10}$ adjusted p values on the y axis. These analytical steps were taken to ensure robust detection of phenotype-associated methylation signatures while minimising false positives.

We investigated CpG targets associated with the phospholipid biosynthesis pathways—identified as altered in the maternal metabolomic data—in cord plasma to validate the upstream biology of metabolic products at the regulatory level comparing the EFG and AG phenotypes. To assess aggregate statistical significance at gene level, we applied the Empirical Brown's method, a statistical approach for combining multiple, potentially correlated p values. In methylation studies, CpG sites mapping to the same gene often show correlated methylation patterns; ignoring this correlation, using standard statistical methods such as Fisher's test, can inflate type I error rates. Results were visualised in original circularised figures to integrate these multiple layers of information.

Genetic association with each of the phenotypes was examined as a dichotomous trait using an additive logistic regression model in the mother–child dyads separately. Newborn sex and the first five genetic principal components were included as covariates. The GWAS were first conducted in each genetically homogenous subgroup. After excluding subgroups with few samples, six subgroups with different genetic ancestries were included in the GWAS analysis. GWAS summary statistics from these six subgroups were pooled using a fixed-effects, inverse-variance weighted meta-analysis.

We report the crude GWAS p values, but we adjusted the significance thresholds to account for multiple testing to 5×10^{-8}. As we conducted ten GWAS tests for both maternal and fetal associations across the five phenotypes, a more stringent significance threshold was required ($5\times10^{-8}/10$).

We summarised maternal and neonatal characteristics, and we compared the EFG phenotype with all other phenotypes combined using n (%) and χ^2 for categorical variables and mean (SD) and *t* tests for continuous variables. The MGT phenotype was the reference group for comparisons with the other four phenotypes: linear regression models to calculate β coefficients and 95% CIs for continuous variables, and Poisson regression models with a log-link function and robust SEs to calculate relative risk and 95% CI for categorical variables. All analyses were performed using R (version 4.2.1) and STATA (version 17.0).

Role of the funding source

The funder of the study had no role in study design, data collection, data analysis, data interpretation, or writing of the report.

Results

Characteristics of the five fetal cranial growth phenotypes

We have previously described five cranial growth phenotypes (EFG, LFG, MGT, AG, and LMG) with distinct neonatal, postnatal head circumference, length and height, weight, and scores for cognition, behaviour, language, vision, and fine motor skills at age 2 years.[9] Compared with the international standards and expressed as z-scores,[5,20,27,28] the EFG phenotype had: (1) reduced growth velocity for head circumference and for femur length (appendix 1 pp 15–16) by 20 weeks' gestation; (2) lower postnatal mean values of head circumference up to age 2 years; (3) the lowest adjusted mean β coefficient scores for height at age 2 years; and (4) the lowest developmental domains at age 2 years with highest vision reduction coefficients.[9] The appendix 1 (pp 21–26) shows a summary of the previously reported maternal and neonatal characteristics and outcomes of these phenotypes.[9]

Using novel methodology,[8] we estimated total brain volume (TBV) across the five phenotypes, expressed as z-scores of the international standard, between 14 and 31 weeks' gestation (ie, the window during which the phenotypes diverged; appendix 1 p 15). The TBV z-scores were consistently lower in the EFG phenotype than in the other four phenotypes (appendix 1 p 15).

We performed sensitivity analyses comparing the maternal baseline characteristics, and pregnancy and neonatal outcomes, of all women eligible for 3D ultrasound and blood sampling (n=2111) with the final analytical subset used for TBV estimation (n=1569). Both subsamples were nearly identical with respect to those parameters supporting the representativeness of the analytical sample (appendix 1 p 34).

The prevalence of small for gestational age (SGA; birthweight <10th centile)[27] was 29·3% (n=98) in the EFG phenotype, which was higher than for the MGT (11·5%, n=182) and the LFG (8·7%, n=18) phenotypes, and considerably higher than the LMG (3·7%, n=8) and AG (2·0%, n=6) phenotypes, suggesting a "dose-effect" association according to the degree of cranial and brain growth (appendix 1 p 25).

Uterine artery, umbilical cord blood flow, and placental histopathology

Umbilical artery Doppler Pulsatility Index (PI) trajectories from 22 weeks' gestation differed among the phenotypes.

The mean value before 24 weeks' gestation for the EFG phenotype was above +1SD of the standards,[29] indicating decreased feto-placental perfusion, and remained higher than the other phenotypes during the third trimester of pregnancy (appendix 1 p 17). However, the mean values in the Doppler PIs of the uterine arteries were similar across the phenotypes (appendix 1 p 17). The combination of raised resistance in the umbilical arteries with normal maternal uterine artery flow is indicative of feto-placental dysfunction rather than diminished maternal blood supply.

The appendix 1 (p 17) shows the prevalence of placental vascular malperfusion in the five phenotypes (n=1014). The prevalence of maternal vascular malperfusion was 18·1% in the EFG phenotype, higher than in the other phenotypes (around 5%; p<0·001). Such lesions occur in association with preeclampsia, preterm birth, and intrauterine growth restriction (IUGR).[30] The rates of fetal vascular malperfusion were similar across all five phenotypes.

Thus, the EFG phenotype is exposed to an abnormal placental environment with reduced blood and nutrient transfer, starting likely in the first trimester of pregnancy due to alterations in placental structure and blood flow.

Maternal and fetal genetic variants

We conducted a GWAS of the early maternal and umbilical cord samples to look for genetic variants associated with the phenotypes. For the EFG phenotype, there were only two significant GWAS (p values adjusted for multiple comparisons) in the maternal samples on chromosome 16 near *TMEM114* (index SNP: rs78913226, $p=6\cdot44\times10^{-8}$) and umbilical cord samples on chromosome 3 near *CNTN6* (index SNP: rs2678251, $p=1\cdot32\times10^{-7}$; appendix 1 p 18). Neither gene was involved in any of the metabolic pathways reported in this paper; however, *CNTN6* copy number variations were associated with neurodevelopmental behavioural disorders.[31]

Thus, there was little evidence of maternal or fetal genetic variants, at a preselected GWAS significance level of $p<5\times10^{-8}$, that could explain the phenotypes.

Maternal early pregnancy metabolomic markers

Figure 1 presents volcano plots of OR distributions for the metabolite signatures, according to p value, adjusted by maternal age and newborn sex, across the five phenotypes. The MGT phenotype was associated with the least metabolic activity, with limited variability and no significant metabolite signatures in maternal plasma. Conversely, the EFG phenotype had 602 significant signatures at the p value threshold of 1×10^{-6}: 436 with positive OR and 166 with negative OR. Hence, only maternal early pregnancy metabolites in the EFG phenotype are presented in table 1 and table 2.

The appendix 1 (p 19) shows the results of a supervised UMAP using the significant metabolites from maternal

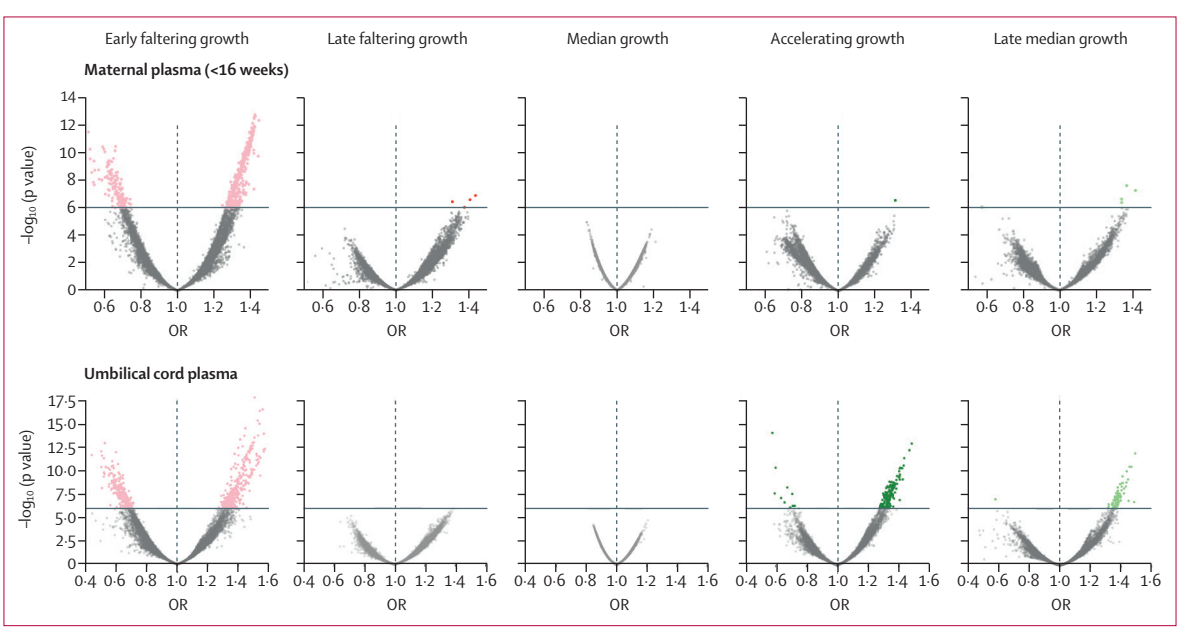

Figure 1: **Volcano plots of OR distributions across the five fetal cranial growth phenotypes for all metabolite signatures in maternal early pregnancy and umbilical cord samples, according to p value**

ORs adjusted by maternal age and newborn sex. Dots indicate $p<1\times10^{-6}$ signatures. (A) Maternal early pregnancy plasma samples. For the early faltering growth phenotype, there were 166 metabolite signatures with reduced OR and 436 metabolite signatures with increased OR (represented by pink dots). (B) Umbilical cord plasma samples at birth. For the early faltering growth phenotype, there were 255 metabolite signatures with reduced OR and 334 metabolite signatures with increased OR (pink dots). For the accelerating growth phenotype, there were 11 metabolite signatures with reduced OR and 140 metabolite signatures with increased OR (green dots). OR=odds ratio.

and cord plasma associated with the EFG and AG phenotypes, that diverged most at the metabolome-wide level. The data separated into two clusters, indicating visually distinctive underlying metabolite abundance profiles between the EFG and AG phenotypes in maternal and cord plasma.

We prioritised the most significant signatures in figure 1 for molecular characterisation and identification in a subsequent mass spectrometry experiment. Those selected had a p value lower than 1×10^{-8} and median abundance level of more than 500 counts (88 species with positive OR and 20 species with negative OR; if referring to the polarity of the detected species, there were 71 in positive mode and 37 in negative mode). Of those with adequate peak quality and spectra, we characterised 25 unique metabolites significantly associated with the EFG phenotype (20 positive and five negative). Where metabolite species are identifiable, this was done using the MS/MS data.

Table 1 presents the chemical structures of the species characterised in maternal plasma from the EFG phenotype (post-lipid class numbering represents carbon acyl-chain length and unsaturation), as well as their mass-to-charge ratio, OR, and p values associated with the probability of belonging to that phenotype.

Phosphatidylcholines (PCs) were the most associated signature, of which 11 were most likely individual molecules (nine positive and two negative OR). These PCs had at least one polyunsaturated fatty acyl (PUFA; ie, ≥two double bounds) side chain. There were a further two phosphatidylethanolamine (PE) species, and one lysophosphatidylcholine (LPC; 18:3 [ie, 18 carbon atoms and three double bonds]), all with PUFA acyl-chains. These PC, PE, and LPC species were positively associated with the EFG phenotype (table 1).

The EFG phenotype was also associated with ten ether lipid species in maternal plasma (table 2). Eight had an alkyl chain attached by an ether bond (O- prefix)—ie, ether lipids, but only the non-oxidised alkenyl chain (PC [P-16:0_22:5]), and the PC(P16:0;O2_18:1) were plasmalogens. All were positively associated with the EFG phenotype, except for PC(O-20:5;O3_16:0), which was negatively associated.

No maternal early pregnancy metabolite signatures were identified in the AG phenotype (figure 1). Nevertheless, we used the same maternal samples to compare the most significant EFG metabolites with those previously identified in the abdominal EFG and AG phenotypes, based on serial measurements of the fetal abdominal circumference.[10] The comparison was possible because phenotyping used the same cohorts and laboratory techniques, with identical sampling, metabolomic methods, and analytical strategy.

Figure 2 and the appendix 1 (p 27) present 14 overlapping compounds characterised in the three phenotypes with an enriched representation of oxidised PCs. There were two non-oxidised canonical PCs, 11 oxidised canonical PCs, and 5-hydroxyeicosatetraenoic acid (5-HETE), putatively assigned by MS/MS, which is an eicosanoid derivative of PUFA side-chains. All lipids contained a

	p value	OR (95% CI)	m/z
Canonical PCs			
PC (18:1/18:2)	$1{\cdot}15\times10^{-22}$	1·42 (1·32–1·51)	784·58
PC (16:0/22:6)	$2{\cdot}23\times10^{-12}$	1·42 (1·32–1·51)	806·57
PC (18:2/18:2)	$1{\cdot}36\times10^{-11}$	1·40 (1·30–1·49)	782·57
PC (16:1/20:4)* or PC (16:0/20:5)	$1{\cdot}59\times10^{-11}$	1·40 (1·30–1·49)	780·55
PC (16:1/20:4)*	$5{\cdot}55\times10^{-9}$	1·33 (1·23–1·42)	794·58
PC (16:0/20:5) or PC (16:1/20:4)	$1{\cdot}82\times10^{-11}$	1·39 (1·30–1·49)	780·55
PC (14:0/20:4)	$2{\cdot}81\times10^{-9}$	1·34 (1·24–1·43)	754·54
PC (14:0/22:6)	$3{\cdot}85\times10^{-9}$	0·64 (0·78–0·49)†	778·54
PC (18:2/16:1)	$8{\cdot}66\times10^{-9}$	0·63 (0·79–0·48)†	756·55
Oxidised PCs (PC;O)			
PC (18:2;O/18:0) or PC (O-18:02/18:3)	$1{\cdot}79\times10^{-12}$	1·41 (1·32– 1·50)	802·59
PC (40:7;O2)	$3{\cdot}16\times10^{-12}$	1·41 (1·31–1·50)	864·57
PEs			
PE (18:0/20:4)	$1{\cdot}75\times10^{-13}$	1·42 (1·33–1·51)	766·53
PE (20:4/18:1) or PE (22:5/16:0)	$1{\cdot}75\times10^{-12}$	1·41 (1·31–1·50)	764·53
LPCs			
LPC 18:3	$3{\cdot}56\times10^{-12}$	1·40 (1·31–1·49)	540·31

m/z is a standard unit in mass spectrometry indicating the mass of an ionised molecule divided by its charge. ORs represent the association with the cranial EFG phenotype, adjusted for maternal age and newborn sex. Models are adjusted for maternal age and newborn sex; post-lipid class numbering represents carbon acyl-chain length and unsaturation. EFG=early faltering growth. OR=odds ratio. LPC=lysophosphatidylcholines. m/z=mass-to-charge ratio of an ion. PC=phosphatidylcholine. PE=phosphatidylethanolamine. *Structural isomers with different retention times. †Negatively associated.

Table 1: **Early pregnancy total maternal lipid species exclusively associated with fetal cranial EFG phenotype (n=335)**

	p value	OR (95% CI)	m/z
Alkyl-acylphospholipids PC(O-)			
PC (O-18:3;O3/16:0); PC (P-18:2;O3/16:0); PC (O-16:0;O2/18:3;O)	$1{\cdot}42\times10^{-12}$	1·42 (1·33–1·52)	790·56
PC (O-20:4;O3/18:1); PC (P-20:3;O3/18:1); PC (O-22:7;O3/16:0)	$3{\cdot}06\times10^{-12}$	1·41 (1·32–1·50)	840·57
PC (O-19:6;O2/17:0); PC (P-19:5;O2/17:0); PC (O-16:2;O2/20:4)	$3{\cdot}82\times10^{-12}$	1·41 (1·32–1·51)	796·55
PC (O-14:0;O2/20:4); PC (O-18:4;O2/16:0); PC (P-18:3;O2/16:0)	$9{\cdot}01\times10^{-12}$	1·39 (1·30–1·48)	772·55
PC (O-18:2;O/16:0); PC (P-18:1;O/16:0)	$1{\cdot}62\times10^{-11}$	1·40 (1·30–1·49)	774·56
PC (O-20:5;O3/16:0); PC (P-20:4;O3/16:0)	$4{\cdot}15\times10^{-10}$	0·64 (0·50–0·78)*	814·56
PC (O-18:0;O2/18:3); PC (18:2:0/18:0)	$1{\cdot}79\times10^{-12}$	1·41 (1·32–1·50)	802·59
PC (O-16:1/22:5); PC(O-18:4/20:4);	$1{\cdot}72\times10^{-11}$	1·39 (1·30–1·48)	792·59
Plasmalogens PC(P-)			
PC(P-16:0/22:5); PC(P-18:3/20:4)	$1{\cdot}72\times10^{-11}$	1·39 (1·30–1·48)	792·59
PC(P-16:0;O2/18:1); PC(P-18:1;O/16:0;O); PC(O-16:0;O2/18:2); PC(O-16:2;O2/18:0)	$6{\cdot}80\times10^{-10}$	1·35 (1·26–1·45)	776·57

m/z=mass-to-charge ratio of an ion. m/z is a standard unit in mass spectrometry indicating the mass of an ionised molecule divided by its charge. Models are adjusted for maternal age and newborn sex; post-lipid class numbering represents carbon acyl-chain length and unsaturation. ORs represent the association with the cranial EFG phenotype, adjusted for maternal age and newborn sex. EFG=early faltering growth. OR=odds ratio. *Negatively associated.

Table 2: **Maternal early pregnancy ether lipid species exclusively associated with fetal cranial EFG phenotype (n=335)**

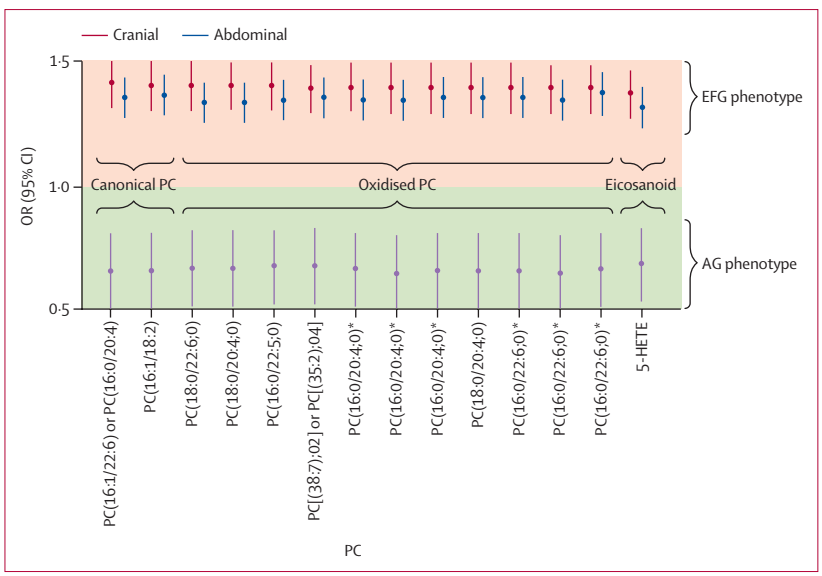

Figure 2: **Associations of the 14 early maternal lipid species overlapping the fetal cranial EFG phenotype with the fetal abdominal circumference EFG and AG phenotypes**
All ORs are significant at the p value <1×10⁻⁶. Models adjusted by maternal age and newborn sex. AG=accelerating growth. EFG=early faltering growth. OR=odds ratio. PC=phosphatidylcholine.

PUFA acyl chain. Importantly, these metabolites were positively associated, with statistical significance, with both EFG phenotypes (ie, cranial and abdominal), but negatively associated, in a reciprocal relationship, with the abdominal AG phenotype.

In short, in the cranial EFG phenotype, there was an over-representation of maternal ether-bonded alkyl-acyl phospholipids (PC-O; rather than plasmalogens) and canonical PC species (rather than PEs). Oxidised PCs were positively associated with both EFG phenotypes, but negatively with the abdominal AG phenotype.

Fetal metabolomics markers

We identified no metabolites exclusive to cord plasma among the MGT and LFG phenotypes that reached our strict criterion of p value lower than 1×10⁻⁶ for significance (figure 1). Of the significant, non-overlapping signatures in cord plasma at the p value threshold of 1×10⁻⁶, we prioritised for molecular characterisation a small number in those in the EFG phenotype (ten in total, of which six were upregulated and four downregulated).

The EFG phenotype showed a positive association in cord samples with (ie, an accumulation of) metabolites involved with fatty acid (FA) transport into the mitochondria for β-oxidation such as carnitine, deoxycarnitine, and octanoylcarnitine, suggesting impaired FA β-oxidation in the EFG phenotype (appendix 1 p 28). This effect is consistent with the hypoxic environment indicated by the placental histopathology. Interestingly, the autosomal recessive medium chain acyl-CoA dehydrogenase deficiency is a FA oxidation disorder, which also manifests with increased octanoyl-carnitine in newborn babies; these children develop acute hypoglycaemia during periods of fasting.[32,33]

Moreover, we identified 33 signatures that overlapped in a reciprocal association between the EFG and AG phenotypes (p<1×10⁻⁶). Of these, 26 were negatively associated (ORs close to 0·5) and seven were positively associated (ORs close to 1·5) with the EFG phenotype. 12 of these signatures could be identified: ten downregulated and two upregulated in the EFG phenotype, with opposite effects in the AG phenotype (figure 3). Octanoylcarnitine (or valproylcarnitine) was upregulated in the EFG but downregulated in the AG phenotype, which are involved in the transfer of long-chain FAs across mitochondrial membranes for β-oxidation. Their accumulation in cord plasma again suggests a reduction in FA β-oxidation in the EFG phenotype.

In summary, we noticed consistent evidence of alteration in fetal FA β-oxidation from cord metabolite signatures that are both exclusive to the EFG phenotype and overlapping, in a reciprocal pattern, between the EFG and AG phenotypes.

Among the signatures associated with only the EFG phenotype in cord plasma, there were two very-long-chain dicarboxylic acids (VLCDCAs) that were downregulated: the hexacosanedioic acid ($C_{26}H_{50}O_4$; OR 0·58 [95% CI 0·42–0·74]) and the tetracosanedioic acid ($C_{24}H_{46}O_4$; 0·52 [0·34–0·70]).

Among the downregulated signatures in the EFG phenotype and upregulated in the AG phenotype presented in figure 3, four were nutritional biomarkers: PC (37:3), a long-chain PC with a PUFA, belonging to the diacylglycerol-phosphocholine sub-family; two hexoses, most likely glucose; and a 2-amino-octanoic acid, an omega-amino FA.

There were also four downregulated compounds related to growth and endocrine maturation in the EFG phenotype, reciprocally associated with the AG phenotype: (1) methyloestradiol (an oestrogen receptor agonist) or androstenedione, an endogenous precursor of testosterone and oestrone with weak androgenic effects; (2) paraxanthine, the predominant metabolite of caffeine or similar infusions, with a strong dopaminergic effect; (3) a structural endogenous isomer of ecgonine, consistently downregulated in the maternal EFG samples also; and (4) hydroxy-chlorothalonil, a metabolite of the toxic fungicide chlorothalonil, which had a similar association with the abdominal EFG phenotype in maternal samples (figure 3).

Conversely, there was upregulation in the EFG phenotype, with a reciprocal downregulation in the AG phenotype, of a signature of the non-essential amino acid, hydroxyproline, the main component of collagen. In response to hypoxia or oxidative stress, collagen is degraded to hydroxyproline, which also serves as a marker of bone resorption.

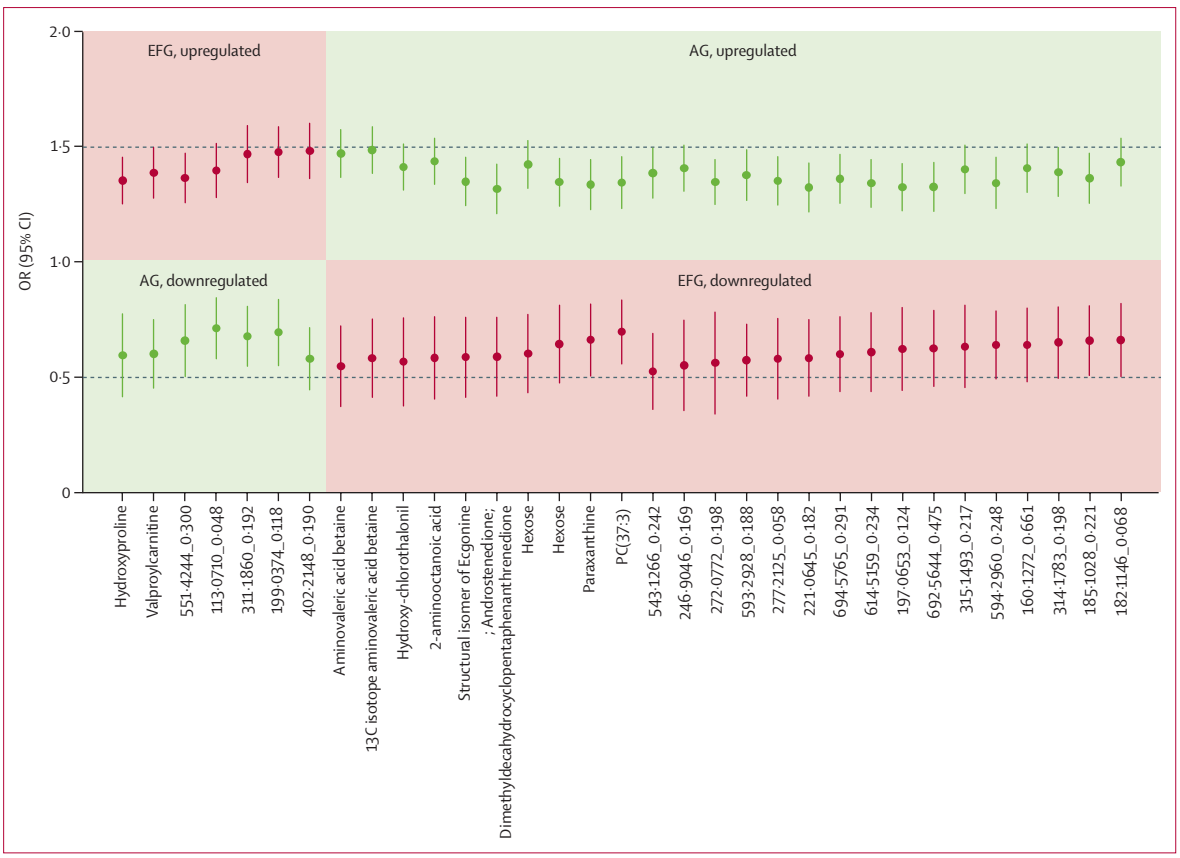

Figure 3: **ORs of the 33 common molecules in umbilical cord samples that overlapped in the fetal cranial EFG and AG phenotypes**
All ORs are significant at the p value $<1\times10^{-6}$. Models adjusted by maternal age and newborn sex. AG=accelerating growth. EFG=early faltering growth. OR=odds ratio.

Fetal epigenetic markers of perturbation of phospholipid biosynthesis in the cranial EFG phenotype compared with the AG phenotype

The total EWAS data showed strong patterns of multiple, predominately hypermethylated CpG sites associated almost exclusively with the EFG and AG phenotypes (figure 4), supporting the metabolomic evidence presented in figure 1.

Therefore, we next focused the analysis on exploring methylation patterns at CpG and gene level, based on the phospholipid biosynthesis pathways altered in the maternal metabolomic data—ie, PC over-representation and plasmalogen deficiency, comparing EFG and AG phenotypes. This analysis evaluated genes encoding enzymes in the glycerophospholipid and plasmalogen pathways, mostly located at the peroxisome and endoplasmic reticulum.

The appendix 1 (p 29) presents a comprehensive methylation landscape of these pathways. The upper part presents results at CpG level demonstrating a consistent downstream pattern, starting with the hypermethylation of predominantly *PEX* genes *10* and *14* that encode proteins directly involved in peroxisome membrane traffic.

We then explored the methylation patterns of genes responsible for the expression of enzymes across the plasmalogen pathway. There were CpGs related to three hypermethylated genes: (1) *FASN*, which encodes FA synthase, a peroxisome multifunctional enzyme, part of the acyl-dihydroxyacetone (DHAP) pathway; (2) *GNPAT*, which encodes glycerophosphatase O-acyltransferase, a peroxisomal membrane enzyme, essential to the synthesis of ether phospholipids; and (3) *TMEM189*, which encodes plasmenyl-ethanolamine desaturase (PEDS1), an endoplasmic reticulum-based enzyme that catalyses the final step in the biosynthesis of plasmalogens (appendix 1 pp 20, 29).

There were also hypermethylated CpGs related to the *PEMT* gene, which encodes the enzyme phosphatidylethanolamine-N-methyltransferase (PEMT), involved in converting PE to PC. Hypermethylation of this key enzyme could be a compensatory reaction to increase PE to balance the metabolomic over-representation of PC (table 1). Conversely, the *FAR1* gene, which encodes fatty acyl-CoA reductase 1, was hypomethylated (appendix 1 pp 20, 29), possibly also as a compensatory mechanism. This enzyme has a key role in the biosynthesis of the FA required to synthesise alkyl-DHAP in the plasmalogen pathway.

We further evaluated the methylation patterns of genes encoding enzymes overlapping with alternative

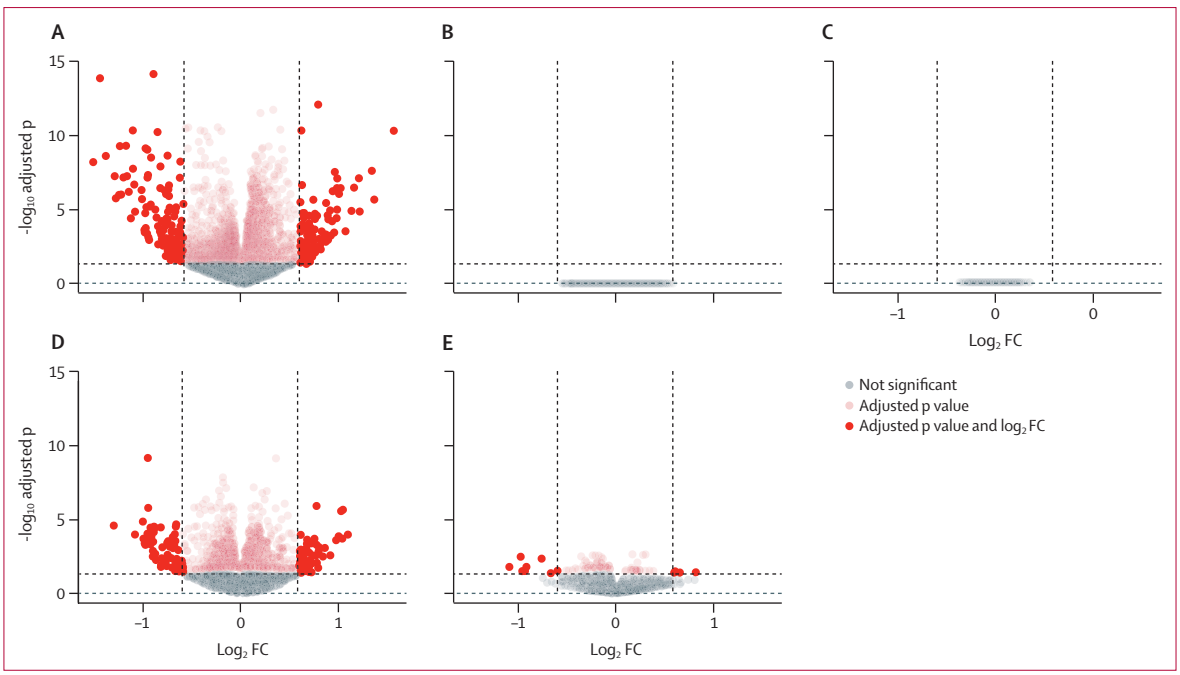

Figure 4: **Volcano plots of Log fold change distributions, according to p value, across the five fetal cranial growth phenotypes from the epigenetic wide association study in umbilical cord samples at birth (n=2377)**

(A) Early faltering growth phenotype. (B) Late faltering growth phenotype. (C) Median growth phenotype. (D) Accelerating growth phenotype. (E) Late median growth phenotype. Dots indicate $p<1\times10^{-6}$ signatures (y axis). Log fold changes (x axis) comparing each specific phenotype (cases) to all other phenotypes (non-cases). FC=fold change.

pathways of phospholipid biosynthesis. We have identified CpG hypermethylation patterns for GPAT and AGPAT, two rate-limiting enzymes and their multiple isomers, a key step for producing phosphatidic acid, shared with the Kennedy pathway, as well as LPIN, PPAP2, PPAPDC1, and PPAPDC3 with their multiple isomers (appendix 1 pp 20, 29). Hypermethylation of genes encoding these enzymes has implications for PE and PC biosynthesis, consistent with the metabolomic results presented in table 1, as well as for triacylglycerols.

This CpG level analysis was complemented by a gene-level analysis focusing on the enzymes related to the pathways explored above. There was consistent hypermethylation of genes described above at the CpG level (eg, *PEX 10* and *PEX 14*, *FASN*, *GNPAT*, and *TMEM189* [PEDS 1 enzyme]; table 3). All are key, underexpressed steps in the biosynthesis of plasmalogens at the peroxisome and endoplasmic reticulum level. *PEMT* was also hypermethylated, suggesting a reduction of PE conversion to PC, and a redirection of the synthesis of PC toward the cytidine 5'-diphosphocholine-choline pathway (table 3).

Among the hypomethylated genes were *FAR 1*, encoding the rate-limiting enzyme in the plasmalogen pathway, and *PEX 6* (table 3). The main function of PEX 6, and its complex of *PEX 16/13/1* genes, is to remove PEX 5 from the peroxisomal membrane to increase peroxisomal transport of proteins.

We specifically explored, at the CpG (appendix 1 p 29) and gene level (table 3), the methylation patterns of *SELEIN* encoding ethanolamine phospho-transpherase (EPT 1) that increases, in the Golgi apparatus, PE expression and de-novo synthesis of plasmalogens. The *EPT 1* gene was hypomethylated (table 3) suggesting again a compensatory increase, at the Golgi apparatus, of PE, which we observed reduced in the metabolomic results (table 1).

The appendix 1 (p 20) presents the methylation status, at CpG and gene level, of the genes selected to compare the EFG and AG phenotypes. In the EFG phenotype, almost all genes related to plasmalogen synthesis, and pathways associated with the biosynthesis of PE or PC, are hypermethylated. These epigenetic data are consistent with our metabolomic results, namely decreased plasmalogens (table 2) with perturbations in the equilibrium of lipid synthesis away from PE toward PC (table 1).

Comparison of fetal epigenetic markers of perturbed FA β-oxidation in the cranial EFG and AG phenotypes

Based on the metabolomic results (appendix 1 p 32), we compared the methylation patterns of the EFG and AG phenotypes at the CpG and gene level of genes responsible for encoding key enzymes at the mitochondrial membrane transfer level. *CPT1A* (the gene coding the primary enzyme in the carnitine shuttle and rate limiter in β-oxidation) was hypermethylated as

was *ACSL1*, needed to generate fatty acyl-CoA (appendix 1 p 32). Overall, the genes encoding enzymes involved in FA β-oxidation steps in the mitochondrial matrix were hypermethylated; the same applied in the tricarboxylic acid cycle that follows, when comparing the EFG and AG phenotypes (appendix 1 p 33).

Hence, the consistent hypermethylation of *CPT1A* and *ACSL1* suggests the suppression, in the EFG phenotype, of the carnitine shuttle, thereby limiting the rate of FA β-oxidation, consistent with the accumulation of FA β-oxidation intermediates in the EFG phenotype in the metabolomics analysis (appendix 1 p 28). This is followed by the hypermethylation, downstream of the β-oxidation pathway, of FA oxidation and the tricarboxylic acid cycle (appendix 1 p 33).

Discussion

In this large cohort of mother–child dyads, we investigated pathophysiological processes associated with EFG of the fetal cranium and brain, using clinical, ultrasonographic, placental histopathology, genetic, metabolomic, and epigenetic data. We identified, with little contribution from genetic variants, metabolic pathways associated with the EFG phenotype, which first manifests clinically between 20–25 weeks' gestation, resulting in poor early child neurodevelopmental outcomes, vision, and linear growth.

In early maternal plasma (<16 weeks' gestation), we found over-representation of PC-Os (rather than plasmalogens) and canonical PC species (rather than PEs) both positively associated with the EFG phenotype. Oxidised PCs were positively associated with both EFG phenotypes (cranial and abdominal) but negatively associated with the abdominal AG phenotype in a reciprocal manner, suggesting a common maternal biological influence on fetal organ growth.

The EFG phenotype (without ultrasound evidence of brain sparing) was associated with increased resistance in cord blood flow. There was also a higher prevalence of maternal (not fetal) vascular malperfusion, which typically arises from impaired maternal blood supply to the intervillous space, whereas fetal vascular malperfusion reflects primary compromise of the fetal circulation.

Three factors make our results robust: (1) the focused analysis of the fetal EWAS data confirmed the hypermethylation of genes *PEX10* and *PEX14*, with a cumulative, downstream hypermethylation of the genes for several key enzymes of the pathway responsible for plasmalogen biosynthesis, supporting regulatory disruption at the epigenetic rather than genetic level; (2) our results are mostly based on the comparison between the EFG and AG phenotypes (the two most extreme cranial growth patterns) supporting reciprocal regulation of the underlying pathophysiological metabolic processes described; and (3) the epigenetic data in cord samples are entirely consistent with our maternal metabolomic results, namely decreased plasmalogens with perturbations in the equilibrium of lipid synthesis away from PE toward PC.

	Mean log FC	Combined p value*	Chromosome
Hypermethylated			
PEX3	0·00054189	0·01845134	6
PEX10	0·02725871	0·01447818	1
PEX14	0·0762567	$5·6264 \times 10^{-5}$	1
FASN	0·02459285	$8·2297 \times 10^{-5}$	17
GNPAT	0·01039514	0·04186585	1
TMEM189	0·01807207	$1·0941 \times 10^{-8}$	20
CHPT1	0·01819669	0·00301435	12
PEMT	0·03781136	0·01041278	17
AGPAT3	0·03276995	0·01052761	21
AGPAT4	0·05063417	$3·4196 \times 10^{-5}$	6
AGPAT5	0·02144672	0·04148308	8
AGPAT6	0·05006366	$9·2603 \times 10^{-5}$	8
AGPAT9	0·0625271	0·00035403	4
LPIN1	0·01926068	0·00990116	2
LPIN2	0·01792635	0·00426378	18
LPIN3	0·04001427	0·01289134	20
LPPR2	0·00601285	0·00245453	19
PPAP2B	0·00566328	0·00214924	1
PPAP2C	0·15243043	$6·599 \times 10^{-5}$	19
PPAPDC1A	0·01263656	$3·4681 \times 10^{-5}$	10
PPAPDC1B	0·0002322	0·00617744	8
PPAPDC3	0·04489279	0·0008549	9
Hypomethylated			
FAR1	−0·02502533	$8·4695 \times 10^{-5}$	11
PEX6	−0·02939293	$2·7468 \times 10^{-9}$	6
PEX12	−0·00807602	0·00449131	17
PEX13	−0·02223739	0·01665688	2
PEX26	−0·02590768	0·00214512	22
DHRS7B	−0·01909956	0·00201757	17
EPT1	−0·0378862	0·00133548	2
PPAP2A	−0·04802252	0·0324226	5

Fetal cranial early faltering growth phenotype (n=269) compared with the fetal cranial accelerating growth phenotype (n=278). FC=fold change. *Combined p values for the gene-level analysis were estimated using Empirical Brown's method.

Table 3: **DNA methylation patterns of genes associated with phospholipid biosynthesis pathways**

Hence, the EFG phenotype, which results in poor growth and developmental outcomes at age 2 years, results from a complex process involving maternal phospholipid imbalance, increased oxidised PCs, alterations in ether phospholipid biosynthesis, and FA β-oxidation in the fetus, likely reflecting the abnormal placental environment associated with this phenotype.

Our study is unique because a wide range of interrelated clinical, placental blood flow and histopathological, metabolomic, genetic, and epigenetic measures were studied in a large multicentre international cohort of mother–infant dyads with well characterised and

accurately dated pregnancies. Moreover, the children's growth and development (a major component of their phenotypic description) were carefully monitored from early pregnancy to age 2 years. Integrating diverse clinical data across time using standardised z-scores was only possible because of the availability of international growth and neurodevelopmental standards.[5,20,27,28]

However, this study has several limitations. First, metabolomics only produces a snapshot of the biology involved (eg, PCs have a 30-min half-life and measures are made at steady state) rather than reflecting the dynamic process of the maternal–fetal metabolic unit.[34] Second, cord samples are not perfectly representative of the intrauterine exposome, but they are used extensively because fetal samples are difficult to obtain. Third, the labour and delivery process might have affected fetal metabolism that is reflected in the cord metabolite signatures related to intrapartum factors rather than fetal growth. Fourth, we were not able to refine the phenotypes by maternal dietary intake as it was impractical in a study of this size, geographical spread, and complexity to measure maternal dietary intake, either weekly or on 24-h recall. Fifth, the GWAS was not powered to identify genes influencing fetal growth. Sixth, the sn1 and sn2 positions of phospholipids could not be defined, and ether lipid annotation is based on non-ether chain identity. Finally, we only adjusted the models by maternal age and infant sex because the fetal growth standards are not sex-specific. Several other maternal characteristics might be considered confounding variables, but these are, in our conceptual framework, part of the phenotypic definitions as independent variables. We did not control for these (including study site) because it would have resulted in over-adjustment; moreover, these contribute important phenotype-specific information as effect modifiers.

Our 2024 systematic review identified 28 metabolomic studies that assessed the pathophysiology of IUGR and SGA in maternal blood, cord blood, or both.[35] Of the 19 studies using maternal blood, none of which evaluated fetal growth trajectories nor neurodevelopment, only five had samples taken at 20 weeks' gestation or earlier.[36–40] Of the 21 studies in cord blood (references available) only one included postnatal follow-up, and only four had more than 50 newborn babies with IUGR or SGA. Most reported significant differences in amino acids, lysophosphatidylcholines, PCs, and carnitine, although the direction of the association varied.

In our data, the patterns of phospholipid subclasses and species in maternal early pregnancy plasma positively associated with the EFG phenotype, specifically the over-representation of PC canonical phospholipid species and PO(O) phospholipid subclasses rather than PEs, sphingomyelins, or plasmalogens, provide mechanistic insights into the restricted growth and lower neurodevelopmental and vision scores observed in this phenotype. PE concentrations are ten-fold higher than PCs in most tissues except muscle;[41] in the human brain, ether lipids are mainly PEs and to a lesser extent PCs and PC(O-)s.[42] PE plasmalogens are highest in brain myelin, retina, immune cells, sperm, and heart and skeletal muscles,[43–46] and they are important in amino acid homoeostasis.[47] PEs prevent oxidation, rescue neuronal cell death, and determine membrane characteristics;[47] and concentrations are low in Alzheimer's and Parkinson's disease.[41,42,45,48]

A key observation was the characterisation of ether lipid PC(O-) species, rather than plasmalogens, in the EFG phenotype. The role of ether lipids in cell differentiation and signalling pathways is particularly relevant for fetal tissues. Plasmalogens are the most common form of ether lipids in higher order membranes such as myelin, and are reduced in conditions affecting myelination, as well as chronic inflammatory and immune diseases, oxidative stress, ageing, neurodegenerative conditions, Alzheimer's and Parkinson's disease, and respiratory and heart diseases.[44] Plasmalogen reduction or depletion induces compensatory mechanisms, including macrophage activation,[49,50] and a dynamic adaptation of cellular phospholipid composition to exogenous lipid alterations.[51]

We have characterised the ether lipid PC(O-16:1_22:5), which is structurally related to precursors of PAF (acetyl-glyceryl-ether-phosphorylcholine). PAF is produced mostly by cells involved in host defence; it is a potent mediator and modulator of pathological processes and multiple other biological activities.[52]

Oxidised phospholipid species represent the largest component of the pool of characterised metabolites positively associated with both EFG phenotypes (brain, cranial, and abdominal) and negatively with the abdominal AG phenotype, in a consistent reciprocal relationship, supporting an underlying biological phenomenon. Characterisation of 5-HETE, without prostaglandins, suggests a preferential mechanism for the amino acid metabolic pathway (LOX and CYP) that has been positively associated with SGA.[38] Like other eicosanoids, these are hormone-like signalling agents active in upregulating acute inflammatory and allergic responses.

Finally, our epigenetic data demonstrated hypermethylation of *PEX* genes essential for glycerophospholipid biosynthesis enzyme import into the peroxisomal matrix, the basic step in glycerophospholipid production. This hypermethylation of *PEX* genes represents a functional deficiency. Conversely, *PEX16*, responsible for peroxisome membrane assembly (ie, a function unlike other *PEX* genes), was hypomethylated.

Two other genes (*FASN* coding for FAS and *TMEM189* coding for PEDS1) were hypermethylated in the EFG phenotype compared with the AG phenotype. The functional product of *FASN* is a peroxisomal membrane-located, multifunctional enzyme, part of the DHAP pathway, a precursor for ether lipid synthesis.[47] PEDS1 is an endoplasmic reticulum-based enzyme that facilitates

the conversion from 1–0-alkyl to 1–0-(1z alkenyl) to produce PE plasmalogens.[48] This enzyme only uses (in addition to oxygen) PE as substrate, which is underrepresented in early pregnancy maternal plasma.

Interestingly, the gene coding for FAR1, the rate-limiting enzyme in the pathway, was hypomethylated reflecting a feedback mechanism in response to decreased expression of upstream genes and downstream enzymes. For example, *PEX 14* (hypermethylated in our data) knock-out animals increased the expression of FAR1 (hypomethylated in our data).[53]

Hypermethylation in *PEMT* is highly relevant for growth and development because the enzyme accounts for 30% of hepatic conversion of PE into PC and eventual de-novo formation of choline. Thus, PEMT downregulation could be a compensatory mechanism to rebalance PCs and PE that are over-represented and under-represented in our results. PEMT has a central role in maintaining phospholipid balance, and mediating liver health, weight gain, and insulin resistance.[54]

We provide comprehensive maternal, placental, and fetal metabolic and functional insights associated with early human growth and development. Interventions targeted at the biological mechanisms described here should be evaluated for their potential preventive or therapeutic effects.

Contributors

JV, SHK, ZAB, ATP, FCB, and JAB designed the study with input from MF, LCI, MV, and AS. COOT-M, RO, RMcG, FCB, MF, VIC, SM, HCB, MC, JAB, SAN, LCI, and RC oversaw data collection. The data were curated by EOO, LCI, and SR. RC, LCI, AL, and AW coordinated the study. RG, SR, BE, EOO, KAL, REV, GZ, YV, MKW, LJM, AN, NJS, TWC, DLS, LDR, ATP, SHK, and JV had access to and verified the raw data and conducted analyses. JV, SHK, ACA, ATP, RG, DLS, AU, and LDR wrote the first draft of the paper, and all other authors contributed and revised it critically for important intellectual content. All authors approved the final version for publication, and JV had final responsibility for the decision to submit. Funding was acquired by JV and SHK. The following authors had access to the full raw dataset: JV, RG, SR, DLS, LDR, and SHK. The corresponding author had full access to all the data and final responsibility for submitting the paper.

Equitable Partnership Declaration

The authors of this paper have submitted an Equitable Partnership Declaration (appendix 2). This statement allows researchers to describe how their work engages with researchers, communities, and environments in the countries of study. This statement is part of *The Lancet* Group's broader goal to decolonise global health.

Declaration of interests

ATP is supported by the Oxford Partnership Comprehensive Biomedical Research Centre with funding from the National Institute for Health and Care Research (NIHR) Biomedical Research Centre funding scheme. The views expressed herein are those of the authors and not necessarily those of the UK National Health Service, NIHR, Department of Health or any of the other funders. ATP is a Senior Advisor of Intelligent Ultrasound. All other authors declare no competing interests.

Data sharing

To conform to the original study ethics governing data sharing, anonymised data will be made available upon reasonable request for academic use and within the limitations of the informed consent. In line with the ethical consent, requests should be made to the corresponding author, and every request will need to be reviewed by the INTERBIO-21st Consortium Executive Committee. After approval, the researcher will need to sign a data access agreement with the INTERBIO-21st Consortium.

Acknowledgments

This project was supported by a generous grant (OPP49038) from the Bill & Melinda Gates Foundation to the University of Oxford, UK, for which we are very grateful. The epigenetic studies were supported by Elysium Health (New York, NY 10013, USA). We thank the Health Authorities in Pelotas, Brazil; Karachi, Pakistan; Kilifi, Kenya; Nairobi, Kenya; Johannesburg, South Africa; and Oxford, UK; who facilitated the project by allowing these study sites to participate as collaborating centres. The participating hospitals included: Brazil, Pelotas (Hospital Miguel Piltcher, Hospital São Francisco de Paula, Santa Casa de Misericórdia de Pelotas, and Hospital Escola da Universidade Federal de Pelotas); Pakistan, Karachi (Aga Khan Hospital); Kenya, Kilifi (The Kilifi District Hospital); Nairobi, Kenya (Aga Khan University Hospital); South Africa, Johannesburg (Chris Hani Baragwanath Academic Hospital); Thailand, Mae Sot (Maela Wang Pha, and Mawker Thai Clinics); and UK, Oxford (John Radcliffe Hospital). We are extremely grateful to Philips Medical Systems who provided the ultrasound equipment and technical assistance throughout the project. We also thank MedSciNet UK for setting up the INTERBIO-21st website and for the development, maintenance, and support of the online data management system. We thank the parents and infants who participated in the studies and the more than 200 members of the research teams who made the implementation of this project possible. Finally, we acknowledge the contributions of all the members of the INTERBIO-21st Committees and the local investigators listed in the appendix 1 (p 35). Special acknowledgements are due to Prof Cesar Victora, now retired from the Project, whose contributions to the conceptualisation and realisation of this project have been invaluable, and to Prof Katrin Watschinger and Prof Johannes Berger for their support in the understanding of the phospholipid pathways.

References

1 Bhutta ZA, Das JK, Rizvi A, et al, and the Lancet Nutrition Interventions Review Group, the Maternal and Child Nutrition Study Group. Evidence-based interventions for improvement of maternal and child nutrition: what can be done and at what cost? *Lancet* 2013; **382:** 452–77.

2 Wild CP. Complementing the genome with an "exposome": the outstanding challenge of environmental exposure measurement in molecular epidemiology. *Cancer Epidemiol Biomarkers Prev* 2005; **14:** 1847–50.

3 Villar J, Papageorghiou AT, Pang R, et al, and the International Fetal and Newborn Growth Consortium for the 21st Century (INTERGROWTH-21st). The likeness of fetal growth and newborn size across non-isolated populations in the INTERGROWTH-21st Project: the Fetal Growth Longitudinal Study and Newborn Cross-Sectional Study. *Lancet Diabetes Endocrinol* 2014; **2:** 781–92.

4 Villar J, Puglia FA, Fenton TR, et al. Body composition at birth and its relationship with neonatal anthropometric ratios: the newborn body composition study of the INTERGROWTH-21st project. *Pediatr Res* 2017; **82:** 305–16.

5 Papageorghiou AT, Ohuma EO, Altman DG, et al, and the International Fetal and Newborn Growth Consortium for the 21st Century (INTERGROWTH-21st). International standards for fetal growth based on serial ultrasound measurements: the Fetal Growth Longitudinal Study of the INTERGROWTH-21st Project. *Lancet* 2014; **384:** 869–79.

6 WHO Working Group on Infant Growth. An evaluation of infant growth: the use and interpretation of anthropometry in infants. *Bull World Health Organ* 1995; **73:** 165–74.

7 Villar J, Fernandes M, Purwar M, et al. Neurodevelopmental milestones and associated behaviours are similar among healthy children across diverse geographical locations. *Nat Commun* 2019; **10:** 511.

8 Namburete AIL, Papież BW, Fernandes M, et al. Normative spatiotemporal fetal brain maturation with satisfactory development at 2 years. *Nature* 2023; **623:** 106–14.

9 Villar J, Gunier RB, Tshivuila-Matala COO, et al. Fetal cranial growth trajectories are associated with growth and neurodevelopment at 2 years of age: INTERBIO-21st Fetal Study. *Nat Med* 2021; **27:** 647–52.

10 Villar J, Ochieng R, Gunier RB, et al. Association between fetal abdominal growth trajectories, maternal metabolite signatures early in pregnancy, and childhood growth and adiposity: prospective observational multinational INTERBIO-21st fetal study. *Lancet Diabetes Endocrinol* 2022; **10:** 710–19.

See **Online** for appendix 2

11 Kennedy SH, Victora CG, Craik R, et al. Deep clinical and biological phenotyping of the preterm birth and small for gestational age syndromes: the INTERBIO-21st Newborn Case-Control Study protocol. *Gates Open Res* 2019; **2:** 49.

12 Papageorghiou AT, Kennedy SH, Salomon LJ, et al, and the International Fetal and Newborn Growth Consortium for the 21st Century (INTERGROWTH-21st). International standards for early fetal size and pregnancy dating based on ultrasound measurement of crown-rump length in the first trimester of pregnancy. *Ultrasound Obstet Gynecol* 2014; **44:** 641–48.

13 Perumal N, Gaffey MF, Bassani DG, Roth DE. WHO Child Growth Standards are often incorrectly applied to children born preterm in epidemiologic research. *J Nutr* 2015; **145:** 2429–39.

14 Dewey KG, Cohen RJ, Arimond M, Ruel MT. Developing and validating simple indicators of complementary food intake and nutrient density for breastfed children in developing countries. Final Report. Washington, D.C.: Academy for Educational Development (AED), 2005.

15 WHO Multicentre Growth Reference Study Group. Complementary feeding in the WHO Multicentre Growth Reference Study. *Acta Paediatr Suppl* 2006; **450:** 27–37.

16 de Onis M, Onyango AW, Van den Broeck J, Chumlea WC, Martorell R. Measurement and standardization protocols for anthropometry used in the construction of a new international growth reference. *Food Nutr Bull* 2004; **25** (suppl): S27–36.

17 Sarris I, Ohuma E, Ioannou C, Sande J, Altman DG, Papageorghiou AT, and the International Fetal and Newborn Growth Consortium for the 21st Century (INTERGROWTH-21st). Fetal biometry: how well can offline measurements from three-dimensional volumes substitute real-time two-dimensional measurements? *Ultrasound Obstet Gynecol* 2013; **42:** 560–70.

18 Fernandes M, Stein A, Newton CR, et al, and the International Fetal and Newborn Growth Consortium for the 21st Century (INTERGROWTH-21st). The INTERGROWTH-21st Project Neurodevelopment Package: a novel method for the multi-dimensional assessment of neurodevelopment in pre-school age children. *PLoS One* 2014; **9:** e113360.

19 Murray E, Fernandes M, Newton CRJ, et al. Evaluation of the INTERGROWTH-21st Neurodevelopment Assessment (INTER-NDA) in 2 year-old children. *PLoS One* 2018; **13:** e0193406.

20 Fernandes M, Villar J, Stein A, et al. INTERGROWTH-21st Project international INTER-NDA standards for child development at 2 years of age: an international prospective population-based study. *BMJ Open* 2020; **10:** e035258.

21 Achenbach TM, Rescorla LA. Manual for the ASEBA preschool forms & profiles: an integrated system of multi-informant assessment. Burlington, VT: University of Vermont, Research Center for Children, Youth, and Families, 2000.

22 Adoh TO, Woodhouse JM, Oduwaiye KA. The Cardiff Test: a new visual acuity test for toddlers and children with intellectual impairment. A preliminary report. *Optom Vis Sci* 1992; **69:** 427–32.

23 Agueusop I, Musholt PB, Klaus B, Hightower K, Kannt A. Short-term variability of the human serum metabolome depending on nutritional and metabolic health status. *Sci Rep* 2020; **10:** 16310.

24 Mora S. Nonfasting for routine lipid testing: from evidence to action. *JAMA Intern Med* 2016; **176:** 1005–06.

25 Anderson BJ, Curtis AM, Jen A, et al. Plasma metabolomics supports non-fasted sampling for metabolic profiling across a spectrum of glucose tolerance in the Nile rat model for type 2 diabetes. *Lab Anim (NY)* 2023; **52:** 269–77.

26 Smyth GK. Linear models and empirical Bayes methods for assessing differential expression in microarray experiments. *Stat Appl Genet Mol Biol* 2004; **3:** Article 3.

27 Villar J, Cheikh Ismail L, Victora CG, et al, and the International Fetal and Newborn Growth Consortium for the 21st Century (INTERGROWTH-21st). International standards for newborn weight, length, and head circumference by gestational age and sex: the Newborn Cross-Sectional Study of the INTERGROWTH-21st Project. *Lancet* 2014; **384:** 857–68.

28 de Onis M, Onyango AW, Borghi E, Garza C, Yang H, and the WHO Multicentre Growth Reference Study Group. Comparison of the World Health Organization (WHO) Child Growth Standards and the National Center for Health Statistics/WHO international growth reference: implications for child health programmes. *Public Health Nutr* 2006; **9:** 942–47.

29 Drukker L, Staines-Urias E, Villar J, et al. International gestational age-specific centiles for umbilical artery Doppler indices: a longitudinal prospective cohort study of the INTERGROWTH-21st Project. *Am J Obstet Gynecol* 2020; **222:** 602.e1–15.

30 McBride CA, Bernstein IM, Sybenga AB, McLean KC, Orfeo T, Bravo MC. Placental maternal vascular malperfusion is associated with prepregnancy and early pregnancy maternal cardiovascular and thrombotic profiles. *Reprod Med (Basel)* 2022; **3:** 50–61.

31 Hu J, Liao J, Sathanoori M, et al. CNTN6 copy number variations in 14 patients: a possible candidate gene for neurodevelopmental and neuropsychiatric disorders. *J Neurodev Disord* 2015; **7:** 26.

32 Mason E, Hindmarch CCT, Dunham-Snary KJ. Medium-chain acyl-COA dehydrogenase deficiency: pathogenesis, diagnosis, and treatment. *Endocrinol Diabetes Metab* 2023; **6:** e385.

33 Andresen BS, Dobrowolski SF, O'Reilly L, et al. Medium-chain acyl-CoA dehydrogenase (MCAD) mutations identified by MS/MS-based prospective screening of newborns differ from those observed in patients with clinical symptoms: identification and characterization of a new, prevalent mutation that results in mild MCAD deficiency. *Am J Hum Genet* 2001; **68:** 1408–18.

34 Messias MCF, Mecatti GC, Priolli DG, de Oliveira Carvalho P. Plasmalogen lipids: functional mechanism and their involvement in gastrointestinal cancer. *Lipids Health Dis* 2018; **17:** 41.

35 Conde-Agudelo A, Villar J, Risso M, Papageorghiou AT, Roberts LD, Kennedy SH. Metabolomic signatures associated with fetal growth restriction and small for gestational age: a systematic review. *Nat Commun* 2024; **15:** 9752.

36 Horgan RP, Broadhurst DI, Walsh SK, et al. Metabolic profiling uncovers a phenotypic signature of small for gestational age in early pregnancy. *J Proteome Res* 2011; **10:** 3660–73.

37 Sovio U, Goulding N, McBride N, et al. A maternal serum metabolite ratio predicts fetal growth restriction at term. *Nat Med* 2020; **26:** 348–53.

38 Welch BM, Keil AP, van 't Erve TJ, et al. Longitudinal profiles of plasma eicosanoids during pregnancy and size for gestational age at delivery: a nested case-control study. *PLoS Med* 2020; **17:** e1003271.

39 Morillon AC, Leite DFB, Yakkundi S, et al. Glycerophospholipid and detoxification pathways associated with small for gestation age pathophysiology: discovery metabolomics analysis in the SCOPE cohort. *Metabolomics* 2021; **17:** 5.

40 Voerman E, Jaddoe VWV, Shokry E, et al. Associations of maternal and infant metabolite profiles with foetal growth and the odds of adverse birth outcomes. *Pediatr Obes* 2022; **17:** e12844.

41 Su XQ, Wang J, Sinclair AJ. Plasmalogens and Alzheimer's disease: a review. *Lipids Health Dis* 2019; **18:** 100.

42 Jové M, Mota-Martorell N, Obis È, et al. Ether lipid-mediated antioxidant defense in Alzheimer's disease. *Antioxidants* 2023; **12:** 293.

43 Brites P, Waterham HR, Wanders RJ. Functions and biosynthesis of plasmalogens in health and disease. *Biochim Biophys Acta* 2004; **1636:** 219–31.

44 Bozelli JC Jr, Azher S, Epand RM. Plasmalogens and chronic inflammatory diseases. *Front Physiol* 2021; **12:** 730829.

45 Decandia D, Gelfo F, Landolfo E, Balsamo F, Petrosini L, Cutuli D. Dietary protection against cognitive impairment, neuroinflammation and oxidative stress in Alzheimer's disease animal models of lipopolysaccharide-induced inflammation. *Int J Mol Sci* 2023; **24:** 5921.

46 Fujino T, Yamada T, Asada T, et al. Efficacy and blood plasmalogen changes by oral administration of plasmalogen in patients with mild Alzheimer's disease and mild cognitive impairment: a multicenter, randomized, double-blind, placebo-controlled trial. *EBioMedicine* 2017; **17:** 199–205.

47 Astudillo AM, Balboa MA, Balsinde J. Compartmentalized regulation of lipid signaling in oxidative stress and inflammation: plasmalogens, oxidized lipids and ferroptosis as new paradigms of bioactive lipid research. *Prog Lipid Res* 2023; **89:** 101207.

48 Braverman NE, Moser AB. Functions of plasmalogen lipids in health and disease. *Biochim Biophys Acta* 2012; **1822:** 1442–52.

49 Rubio JM, Astudillo AM, Casas J, Balboa MA, Balsinde J. Regulation of phagocytosis in macrophages by membrane ethanolamine plasmalogens. *Front Immunol* 2018; **9:** 1723.

50 Gaposchkin DP, Farber HW, Zoeller RA. On the importance of plasmalogen status in stimulated arachidonic acid release in the macrophage cell line RAW 264.7. *Biochim Biophys Acta* 2008; **1781:** 213–19.

51 Dorninger F, Brodde A, Braverman NE, et al. Homeostasis of phospholipids - The level of phosphatidylethanolamine tightly adapts to changes in ethanolamine plasmalogens. *Biochim Biophys Acta* 2015; **1851:** 117–28.

52 Montrucchio G, Mariano F, Cavalli PL, et al. Platelet activating factor is produced during infectious peritonitis in CAPD patients. *Kidney Int* 1989; **36:** 1029–36.

53 Guo Y, Zhou P, Qiao L, Guan H, Gou J, Liu X. Maternal protein deficiency impairs peroxisome biogenesis and leads to oxidative stress and ferroptosis in liver of fetal growth restriction offspring. *J Nutr Biochem* 2023; **121:** 109432.

54 Wan S, van der Veen JN, Bakala N'Goma JC, Nelson RC, Vance DE, Jacobs RL. Hepatic PEMT activity mediates liver health, weight gain, and insulin resistance. *FASEB J* 2019; **33:** 10986–95.